IN THE UNITED STATES PATENT AND TRADEMARK OFFICE

In re Application of:		§		
		§		
	Ernest GRIMBERG	§	Confirmation No.:	5035
		§		
Serial No.:	10/567,438	§		
		§		
Filed:	February 7, 2006	§	Group Art Unit:	2884
		§		
For:	Radiometery Using An Uncooled Microbolometer Detector	§		
		§	Attorney Docket:	**31322**
Examiner:	Yara B. GREEN	§		

Commissioner for Patents
P.O. Box 1450
Alexandria, VA 22313-1450

DECLARATION OF GEOFF MELNICK UNDER 37 C.F.R. §1.131

I, Geoff MELNICK, am a patent attorney at Ehrlich & Fenster, Patent Attorneys (formerly Ehrlich & Partners, Patent Attorneys), hereinafter *Ehrlich*.

During August 2003, I prepared an Application that was filed in the Israeli Patent Office as Israeli Patent Application No. 157344 on August 11, 2003, hereinafter *the priority application*.

The Israeli Application serves as the priority document for PCT International Patent Application No. PCT/IL2004/000714, filed on August 3, 2004, hereinafter *the PCT application*. The U.S. was designated in this PCT filing. U.S. Patent Application No. 10/567,438, filed on February 7, 2006 (hereinafter *the instant application*) is the national stage filing of the PCT Application.

I am making this declaration to show that the preparation of the priority application was diligently pursued at *Ehrlich* from just before August 5, 2003, the filing date of

the Allen et al. reference cited by the Examiner, and until August 11, 2003, when the priority application was filed. This time period includes only five work days.

During the time period immediately preceding August 5, 2003 until August 7, 2003, the priority application was undergoing final review by the Applicant, and administrative matters for filing were being handled by *Ehrlich*. Approval for filing was given on Thursday, August 7, 2003 by the Applicant's representative, Mr. Jonathan ZOHN. The Israeli Patent Office and *Ehrlich* were closed on Friday and Saturday, August 8 and 9, 2003. The priority application was filed on Monday, August 11, 2003.

Attached are Exhibits A-C:

1) Exhibit A – An e-mail dated prior to August 5, 2003 (dates blacked out) from Mr. Jonathan Zohn to me, providing a disclosure document that thoroughly shows conception of the subject invention for preparation of the priority application.

1) Exhibit B - An e-mail to me dated August 7, 2003 at 17:14 that includes Mr. Jonathan Zohn's comments, provided on August 7, 2003, 3:11 p.m. to a proposed set of claims for the priority application.

2) Exhibit C – An e-mail dated August 7, 2003 at 19:33 from Mr. Jonathan Zohn to me in which Mr. Zohn approves the revised claims emailed to him at 7:23 p.m. in response to his comments of earlier that day, and approval to file the priority application.

In summary, during the time period from just before August 5, 2003, and until August 11, 2003, I was diligently preparing the previously conceived invention as an Israeli application for filing.

I hereby declare that all statements made herein of my own knowledge are true and that all statements made on information and belief are believed to be true; and further that these statements were made with the knowledge that willful false statements and the like so made are punishable by fine or imprisonment, or both, under Section 1001 of Title 18 of the United states Code and that such willful false statements may jeopardize the validity of the application or any patent issued thereon.

Geoff Melnick

Date: August 17, 2009

Enclosures:

- Exhibits A-C

 Exhibit A

Geoff Melnick

From: Jonathan Zohn [ELOP] [el14012@elop.co.il]
Sent: [redacted]
To: Geoff Melnick
Subject: FW: New Pat Ref: OPG1

Please review the attached and let me know if it is enough for you to prepare a "lean" IL application or a US provisional

I need a budget estimate, including filing and expenses

TODA,
<<UN OPG1 inventor draft 1.doc>>
Jonathan Zohn
Corporate I P Manager
Elbit Systems group

[redacted]

Design Considerations for Radiometer Based on Uncooled Microbolometer Detector

Ernest Grimberg - OPGAL

Abstract

This paper concludes the large effort sustained by OPGAL in designing a radiometer instrument based on the uncooled microbolometer detector. A detailed description of the design considerations, temperature drift model and the expected accuracy is presented. The idea is to enable temperature measurement at a relatively high accuracy for any uncooled microbolometer based FLIR, even if the detector is not a radiometric one, by using the NUC flag as an extremely low frequency chopper.

Keywords : FLIR, Temperature measurement, Uncooled , Microbolometer ,Radiometer, Real time.

1. Introduction

1.1 Opgal manufactures a large number of uncooled microbolometer FLIR cameras, covering a large number of applications. These cameras contain regular uncooled microbolometer detectors that do not contain any radiometric shield. A large amount of these cameras comes with a standard lens of 35mm or 50 mm focal length. The main idea is to upgrade these cameras in order to provide radiometric temperature measurement capability under the restriction of very minor hardware modifications.

1.2 The paper presents the studies performed for developing the measurement concept. The paper presents a relatively detailed model for the energy exchanged among the microbolometer detector and the view, the optics, and the internal camera parts. A mathematical model that describes the detector signal versus target temperature was devised, that would result in a polynomial model for temperature measurement. The paper also presents the solution implemented for reducing the measured temperature drift and the accuracy obtained. There is one major problem not treated in this paper: The two-dimensional modulation transfer function (MTF) influence on the temperature measurements has to be compensated by an inverse filter. This subject is only mentioned in this paper but is not deeply treated.

2. Energy exchanged model

2.1 The video signal at the microbolometer output is generated by the energy exchanged between the detector's elements and:

- The view
- The optics
- The internal camera parts.

The signal itself is built up as a transient process. Assuming that the readout process is interrupted, the energy exchanged takes place until the steady state situation is achieved. The energy exchanged process time constant is equal to the ratio between the suspended structure *Thermal Capacity* and *Thermal Conductance*.

$$\tau = \frac{Thermal\_Capacity}{Thermal\_Conductance} \qquad [\text{sec}]$$

2.2 Assuming an unlimited time interval and assuming that the view can be modeled as a Blackbody radiation source (emissivity=1) the energy exchanged between the detector and the view is expressed by the following formula:

$$P\_view(\Delta Temp)=\frac{\pi\cdot A\_\det}{4(f\#)^2}\int_0^{\infty}\int_{\lambda\_1}^{\lambda\_2}(L(\lambda,Temp_0+\Delta Temp)-L(\lambda,Temp_0))\cdot Trans\_optics(\lambda)\cdot\varepsilon(\lambda)\cdot\exp(-\frac{t}{\tau})dt\cdot d\lambda$$

Equation 1. Energy in joules, exchanged between the detector and the view.

P_view represents the energy [in joules] exchanged between one detector element and the scenery.

$L(\lambda,Temp_0+\Delta Temp)$ represents the view, modeled as an average Blackbody radiation source in Watts/(sr·m^3).

$Temp_0$ represents the detector's suspended structure temperature in degrees Kelvin.

$A\_\det$ represents the effective area of a single detector's element in m^2.

$f\#$ represents optics f number.

λ represents the wavelength in meters.

λ_1 represents the lower integral limit.

λ_2 represents the upper integral limit.

$Trans\_optics(\lambda)$ represents optics transmittance

$\varepsilon(\lambda)$ represents the emissivity of detector's suspended structure.

t presents the time in seconds.

Solving Equation 1 for the *time* variable, the energy exchanged between one detector's element and the view is described by the following expression:

$$P\_view(\Delta Temp)=\frac{\pi\cdot A\_\det\cdot\tau}{4(f\#)^2}\cdot\int_{\lambda\_1}^{\lambda\_2}(L(\lambda,Temp_0+\Delta Temp)-L(\lambda,Temp_0))\cdot Trans\_optics(\lambda)\varepsilon(\lambda)\cdot d\lambda$$

Equation 2. Energy in joules, exchanged between the detector and the view.

Figure 1 describes the energy exchanged between the detector and the view assuming:

- f number equals 1
- high transmittance optics (93%)
- detector emissivity equals 0.8
- effective detector area equaling $(41*10^{-6})^2$ meters
- a spectral band ranging from $8*10^{-6}$ to $12.5*10^{-6}$ meters

2.3 The energy $P\_optics(\Delta Temp)$ exchanged between the detector and optics assuming similar conditions to those described in Paragraphs 2.1 and 2.2 is given by the following mathematical expression:

$$P\_optics(\Delta Temp)=\pi\tau\cdot A\_\det\cdot(\sin(\theta))^2\int_{\lambda\_1}^{\lambda\_2}(L(\lambda,Temp_0+\Delta Temp)-L(\lambda,Temp_0))(1-Trans\_optics(\lambda))\varepsilon(\lambda)d\lambda$$

Equation 3. Energy in Joules, exchanged between the detector and optics.

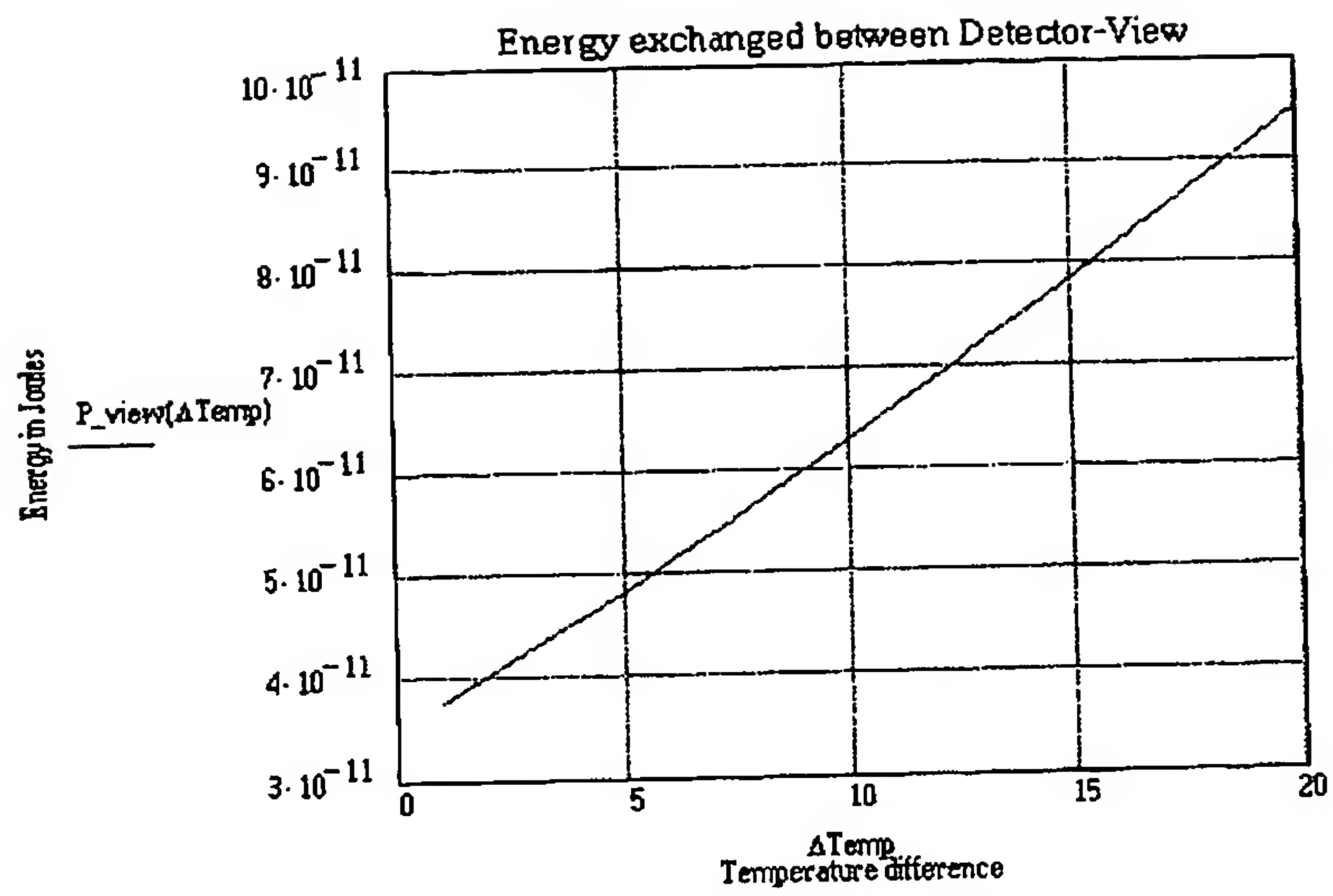

Figure 1. Energy exchanged between detector and view.

$L(\lambda, Temp_0 + \Delta Temp)$ represents the optics, modeled as an average Blackbody radiation source in Watts/(sr·m^3) and emissivity equals $(1 - Trans\_optics(\lambda))$.

$$\theta = arc\_\tan(\frac{1}{2 \cdot f\#})$$

θ represents half of the planar cone angle related to the light collection.

$\theta = 0.464$ radian for f#=1.

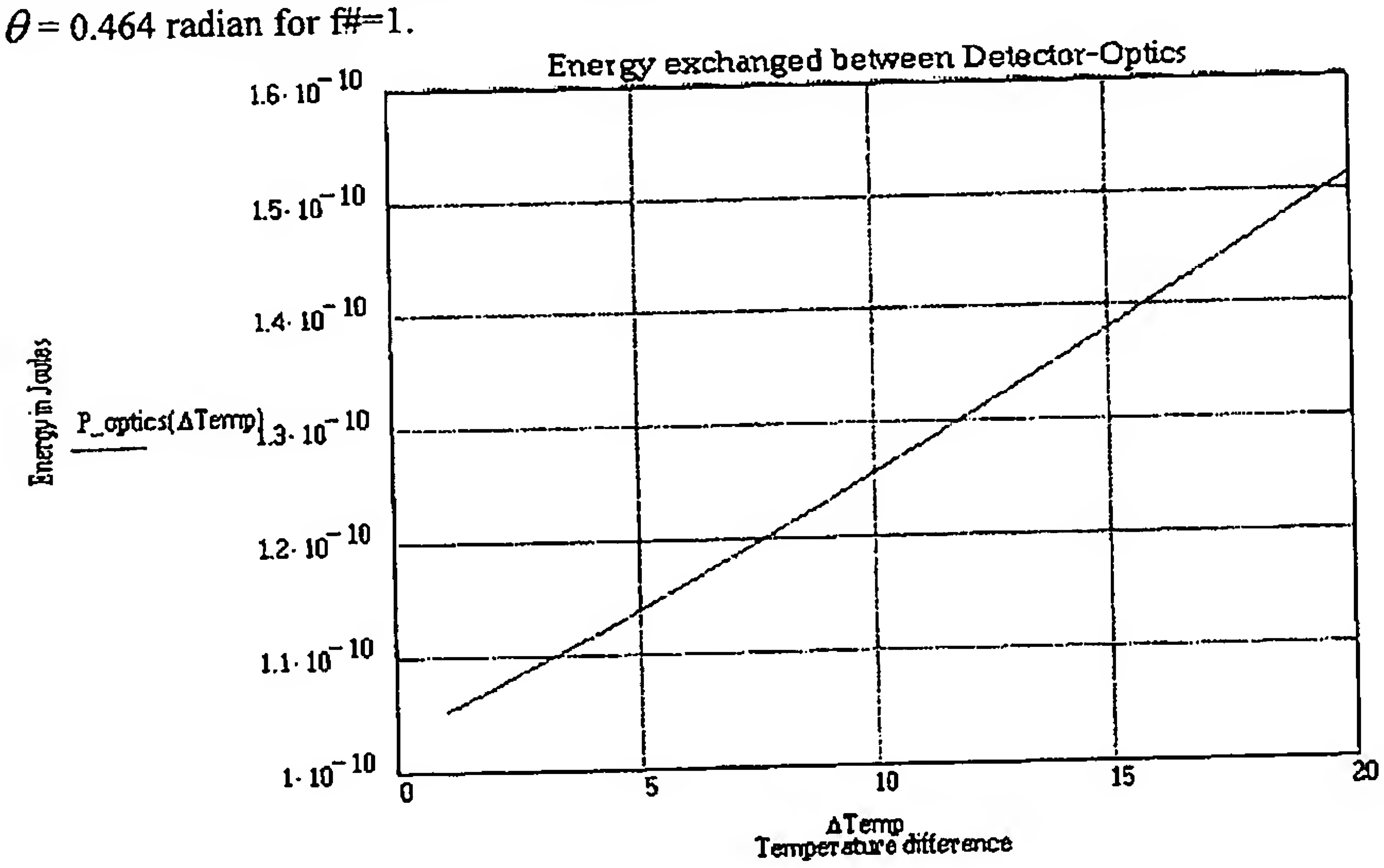

Figure 2. Energy exchanged between the detector and optics.

2.4 The energy $P\_camera(\Delta Temp)$ exchanged between the detector and the internal camera parts assuming similar conditions to those described in the previous paragraphs 2.1, 2.2, and 2.3 is given by the following mathematical expression:

$$P\_camera(\Delta Temp) = \pi\tau \cdot A\_\det \cdot (1-(\sin(\theta))^2) \int_{\lambda\_1}^{\lambda\_2} (L(\lambda, Temp_0 + \Delta Temp) - L(\lambda, Temp_0)) \cdot \varepsilon(\lambda) d\lambda$$

$L(\lambda, Temp_0 + \Delta Temp)$ represents the internal camera parts, modeled as an average Blackbody radiation source in Watts/(sr·m³) and emissivity equals one.

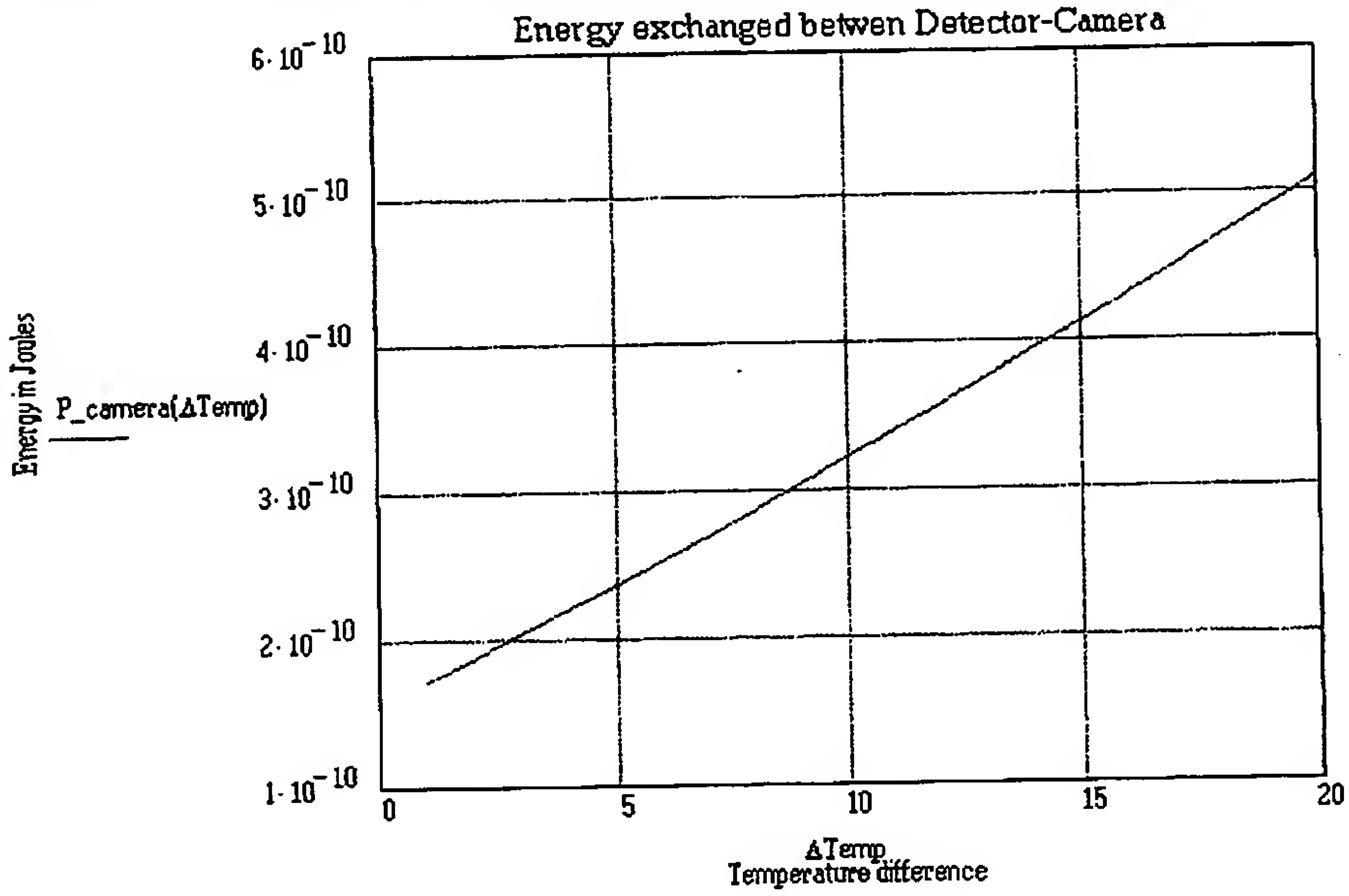

Figure 3. Energy exchanged between detector and internal camera parts.

The energy exchanged between the detector and internal camera parts is the largest one, followed by the energy exchanged between the detector and the optics. The energy exchanged between the detector and the view is the smallest one. Assuming, simultaneously, the same temperature difference between the detector and the view, detector and optics and detector against camera internal parts, the amount of energy exchanged between the detector and the view is about 10%. See figure number 4.

2.5Analysis of the results obtained shows that that the capability to reconstruct the view temperature from the video signal collected is very difficult. The energy exchanged by the detector with the internal camera parts depends on temperature distribution of the internal camera parts. This distribution is not constant, due to the fact that the camera's thermal time constant is very long (about half an hour) and usually the environmental conditions are not stable for such long periods of time. A dynamic model based on the temperature distribution of internal camera parts is too complicated and beyond the capability to be implemented in the existing hardware. Therefore a different solution has to be adopted. The main idea is to use the non-uniformity correction (NUC) update process in order to eliminate the internal camera parts influence. The flag inserted in front of the detector during the NUC update process is used as an extremely low-frequency chopper. The flag's surface facing the detector was treated and coated in order to behave as close as possible as an ideal Blackbody surface. A few very accurate thermistors (±0.025°C) have been installed at the following locations:

2.5.1 One thermistor on the back side of the flag surface

2.5.2 One thermistor on the external surface of detector's vacuum package

2.5.3 Two thermistors have been glued to the external optics metal case.

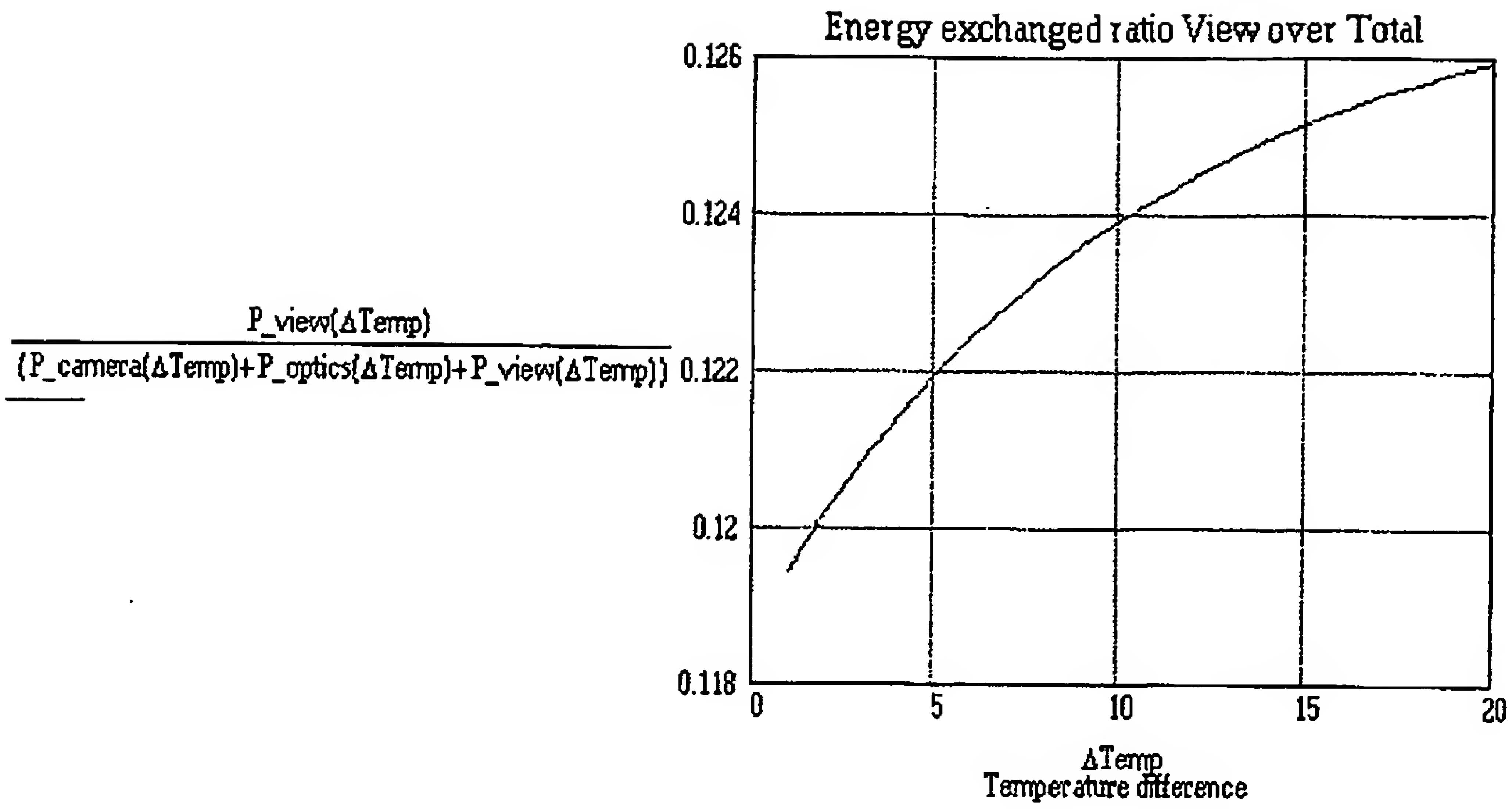

Figure 4. View energy exchanged versus total energy exchanged.

3. Temperature measurement description

3.1 Let us assume, just for simplicity, that the optics influence is negligible. (Later on we shall review this assumption.) Since the NUC update process is periodically performed, we assume that during Process #*n*, the average detector signal As_n (after NUC update and bad pixel replacement (BPR) have been performed) has been calculated. We also assume that during the same NUC updating Process number *n*, the temperature of all the installed thermistors have been acquired.

Tf_n represents the temperature measured on the flag during the *n* NUC update process ,

Td_n represents the temperature measured on the external surface of detector's vacuum package during the number *n* NUC update process,

To_n represents the average temperature measured on the external optics case during the number *n* NUC update process.

Let us assume that the average temperature of some arbitrary, relatively large area of interest (the MTF problem will be mentioned later on) has to be measured. Let us further assume that the specified area belongs to an ideal Blackbody radiation source.

The first approximation of the measured temperature is expressed by Taylor series:

$$T\_mes = T\_mes(As) + \frac{dT\_mes(As)}{dAs}(Sig - As) + \frac{1}{2!}\frac{d^2T\_mes(As)}{dAs^2}(Sig - As)^2 + \frac{1}{3!}\frac{d^3T\_mes(As)}{dAs^3}(Sig - As)^3 \ldots\ldots$$

were: T_mes represents the first approximation of the measured temperature.

Sig represents the average video signal after NUC and BPR of the area of interest mentioned above, at some point in time between the *n* and *n+1* NUC update processes.

We define As to be the average detector signal value measured on the flag during the number *n* NUC updating process. Therefore by definition:

$$T\_mes(As_n) = Tf_n$$

$$T\_mes = F(Sig - As_n) + Tf_n \qquad F(Sig - As_n) = \sum_{l=0}^{\infty} a_l \cdot (Sig - As_n)^l$$

Equation 4. First approximation of the measured temperature

where:

F represents the transform that translates the video signal to temperature.

Equation 4 presents the general idea of using any chopper as a reference source. The chopper's video signal is subtracted from the video signal to be measured. In this way a differential measurement is performed. The video value $Sig - As_n$ is translated to temperature and the offset value Tf_n is finally added. This general approach works very well in the case that As_n and Tf_n are almost constant between successive samples. However, as explained above in paragraph 2.5 this is not the case. The *Error* between the real object temperature and the reconstructed one by the first approximation formula, was plotted versus the temperature measured on the external surface of detector's vacuum package (*Td*) during a period of more than 10 minutes. See Figure 5. The plot described in Figure 5 shows a typical behavior. Figure 6 describes the minimum mean square error linear fit to the *Error* value. However, the slope of the linear best fit is not constant in time. A high slope value means that the camera is far from thermal steady state situation and a very low slope means that the camera is in thermal equilibrium.

3.2 Each time the NUC update procedure is performed, the error of the measured temperature *T_mes* caused by the internal camera temperature fluctuations is eliminated. The typical behavior described in Figure 5 and Figure 6 suggests that by adding an additional term to the first approximation (Equation 4) a better solution will be obtained.

$$T\_mes = F(Sig - As_n) + Tf_n + \frac{\Delta T\_mes_n}{\Delta Td_n}(Td - Td_n)$$

Equation 5

where Td_n represents the temperature measured on the external surface of detector's vacuum package during the *n* NUC update process.

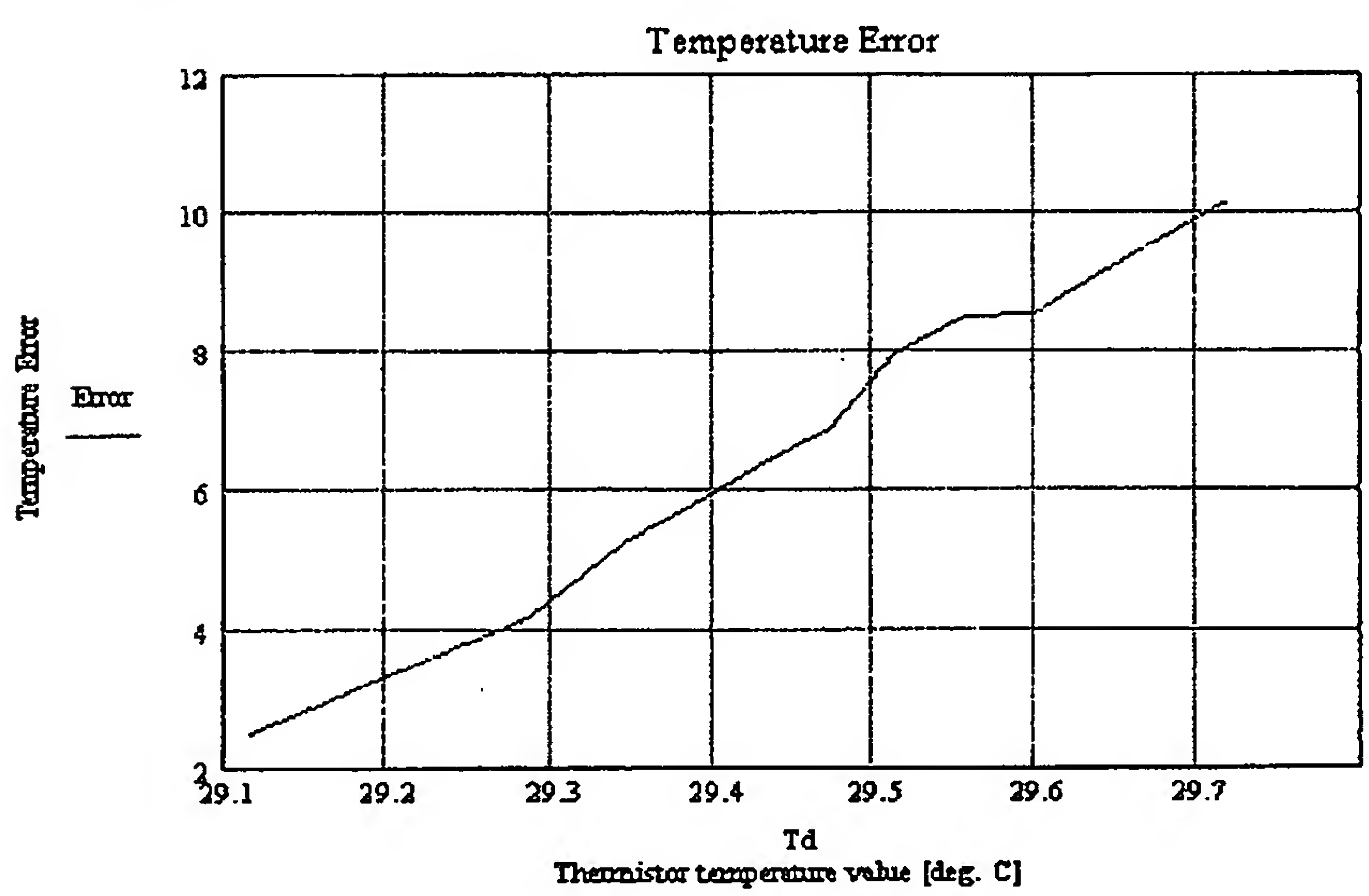

Figure 5. Temperature error versus vacuum package thermistor temperature.

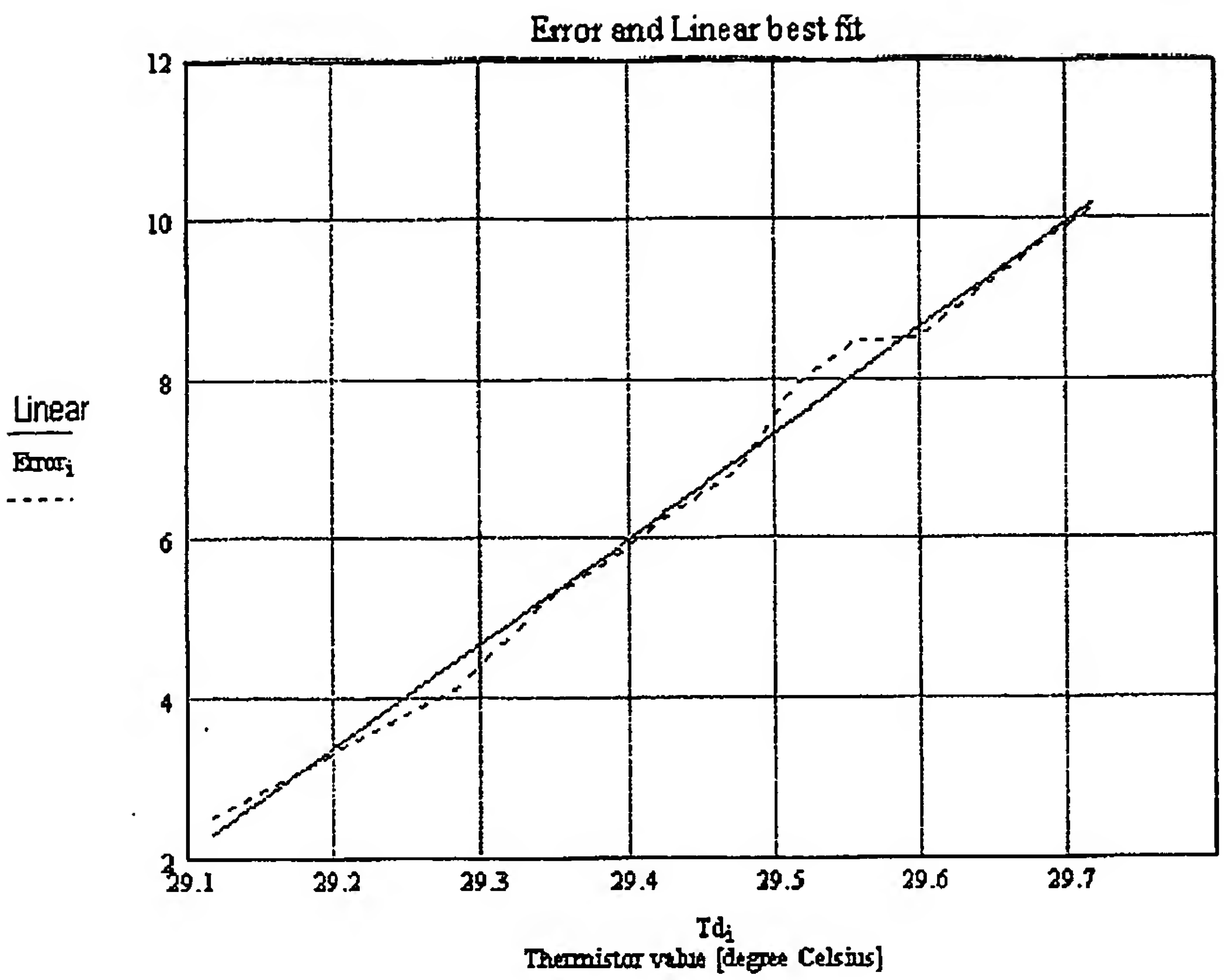

Figure 6. Linear best fit to the *Error* value.

The general idea expressed in Equation 5 cannot be directly implemented. An approximation of this idea was implemented using the values As_n, Tf_n and Td_n, producing Equation 6:

$$T\_mes = F(Sig - As_n) + \frac{F(As_n - As_{n-1}) - (Tf_n - Tf_{n-1})}{Td_n - Td_{n-1}}(Td - Td_n) + Tf_n$$

Equation 6. Second Approximation.

The expression $F(As_n - As_{n-1})$ estimates the total flag change in temperature measured by the detector. However this value contains the error caused by the internal camera parts change in temperature and the real change of flag's temperature.

3.3 This paragraph deals with F function approximation. A mathematical model that describes the detector's signal after NUC and BPR processes was built, in order to estimate the capability to translate the signal to temperature. Figure 7 describes the output of the mathematical model. This mathematical model was used in order to investigate the accuracy that can be obtained using minimum mean square error polynomial approximation to the modeled video signal. For a relative small dynamic range of about 60 degrees Celsius a second order polynomial expansion gives an acceptable accuracy. For example, a second order polynomial expansion is adequate in order to model the optics contribution to the video signal. The third order polynomial approximation covers, with an acceptable error, a range of 300 degrees Celsius, while the fourth polynomial approximation spans a range of about 400 degrees Celsius.

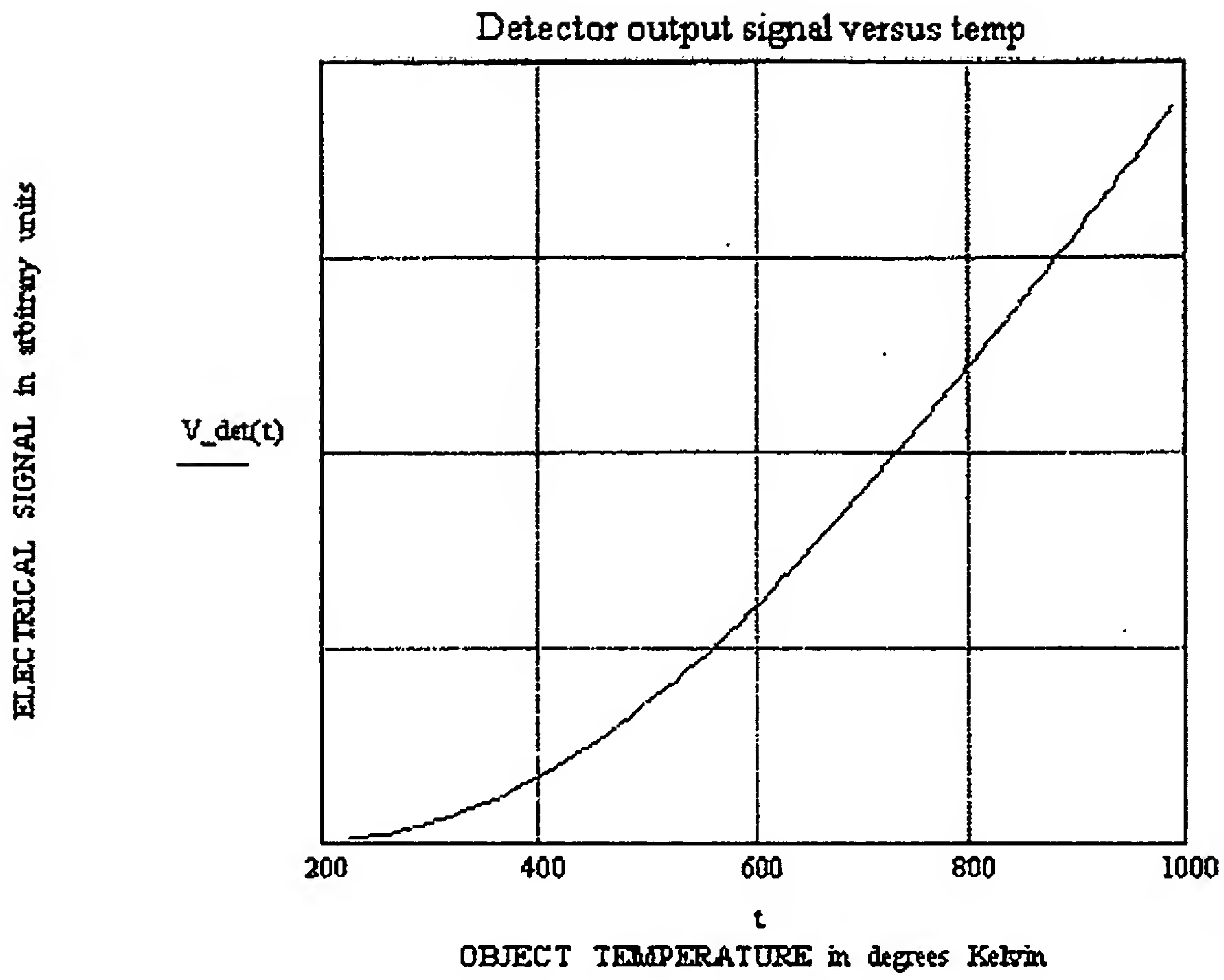

Figure 7. Video output mathematical model

The minimum mean square error polynomial expansion of order L that samples the data at Q different values, requires the solution of $L+1$ linear set of equations. However, the arithmetic used in order to solve the linear set of equations has to be carefully chosen. The minimum number included in the linear set of equations is Q, while the largest number is $\sum_{i=1}^{Q} Sig_i^{2L}$. The graphs presented in Figure 8, Figure 9, and Figure 10 have been calculated using high arithmetical accuracy. A practical solution might be to divide the temperature range into a number of small regions (including some small overlap between the regions), using a lower-order polynomial expansion at each region. Up until this point we neglect the optics temperature influence. The next paragraph describes the solution adopted by Opgal in order to deal with the optics temperature influence.

3.3 The temperature second approximation described in Equation 6 is based on the existence of function F that translates the detector signal to temperature.

$$T\_mes = F(Sig - As_n) + \frac{F(As_n - As_{n-1}) - (Tf_n - Tf_{n-1})}{Td_n - Td_{n-1}}(Td - Td_n) + Tf_n \qquad F(Sig - As_n) = \sum_{l=0}^{\infty} a_l \cdot (Sig - As_n)^l$$

Equation 7.

As was explained in paragraph 2.3 the amount of energy exchanged between the detector and the optics is not negligible. Assuming that the optics temperature influence can be expressed by a polynomial expansion of order R and assuming that the detector signal translation to temperature can be described by a polynomial expansion of order L, the most general form of function F is given by:

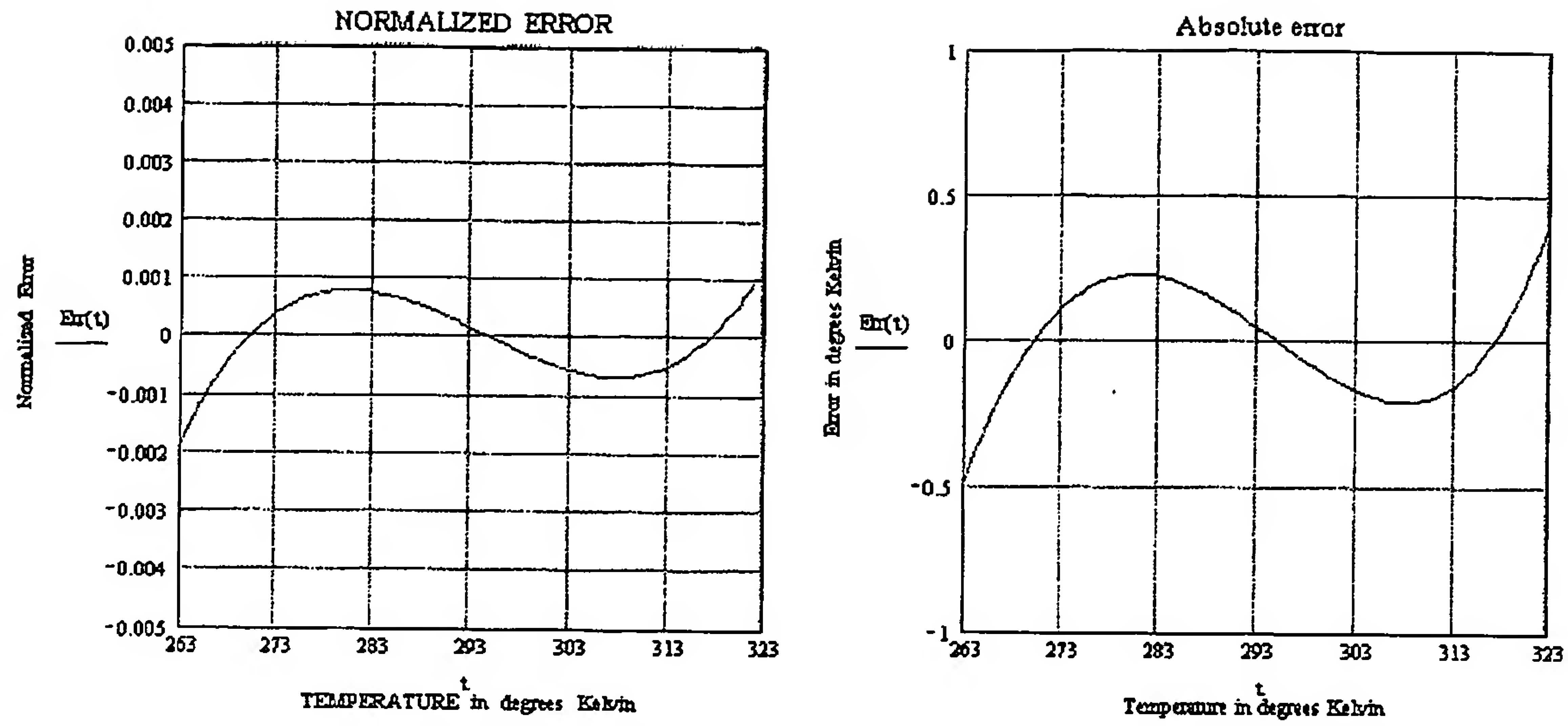

Second order polynomial expansion

Second order polynomial expansion

Figure 8. Second order polynomial approximation.
The normalized error is shown at left, the temperature error at right.

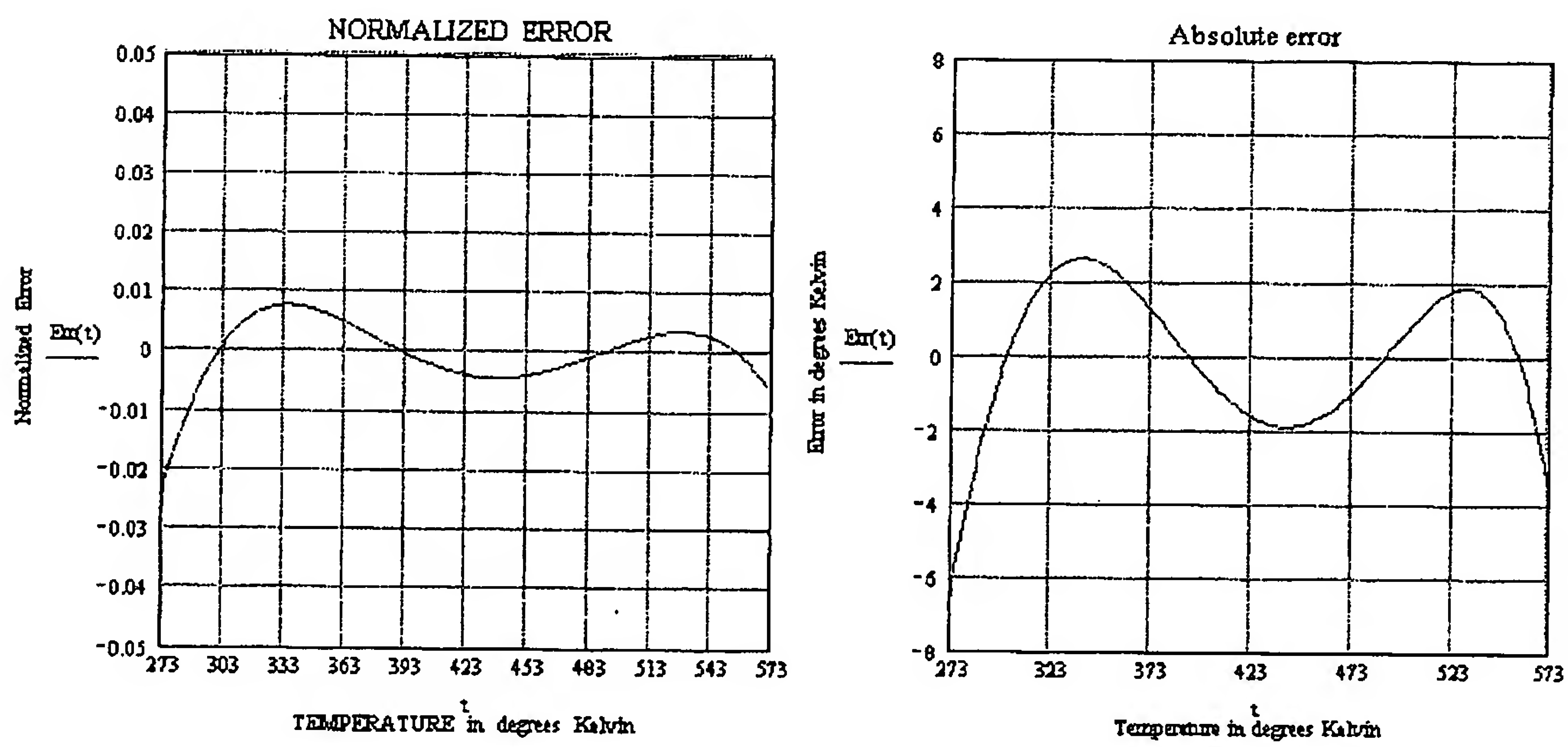

Third order polynomial approximation

Third order polynomial approximation

Figure 9. Third order polynomial approximation.
The normalized error is shown at left, the temperature error at right.

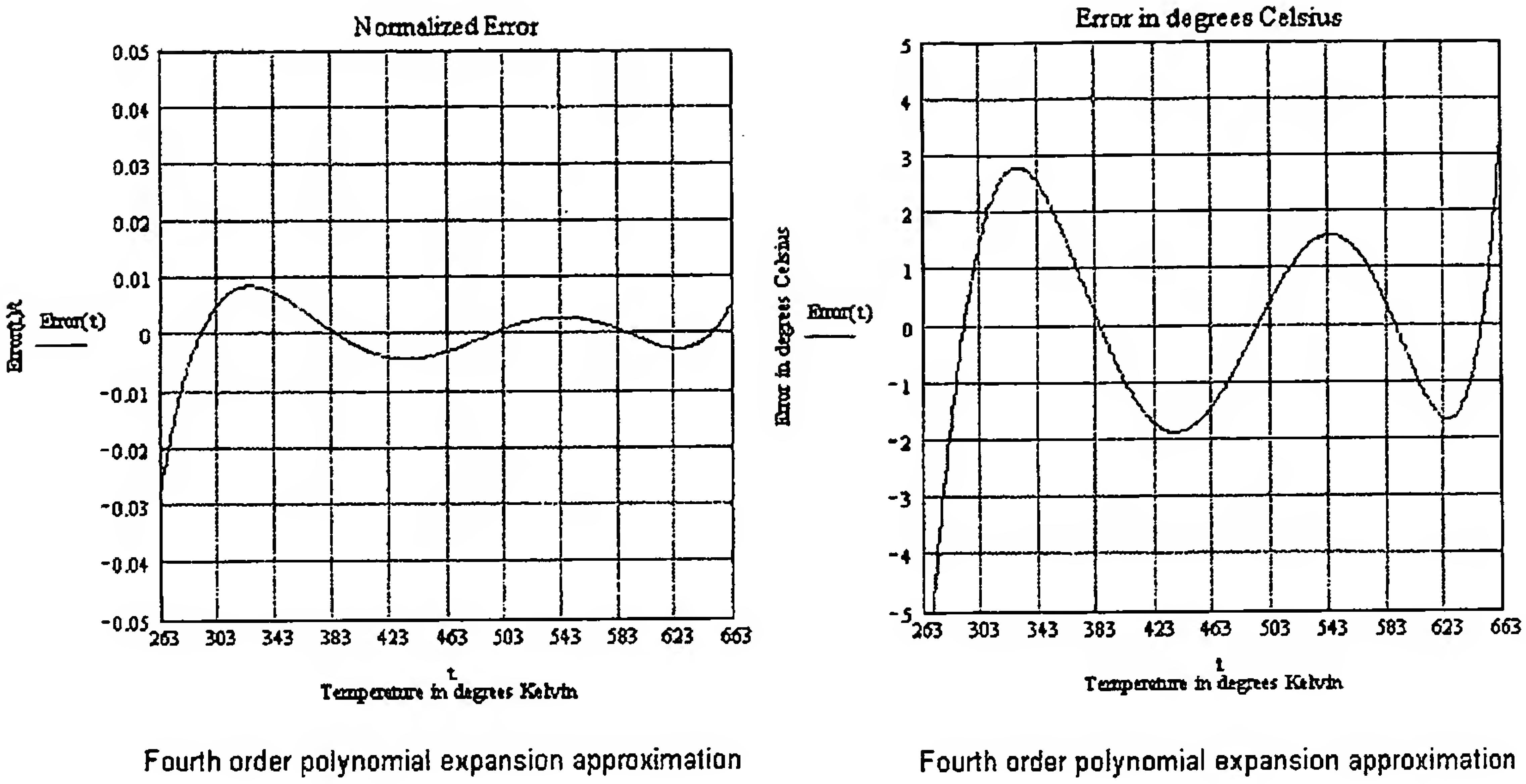

Figure 10. Fourth order polynomial approximation. The normalized error is shown at left, the temperature error at right.

$$F(Sig,To) = \sum_{l=0}^{L}\left(\sum_{r=0}^{R} a_{r,l} \cdot To^{r}\right)Sig^{l} \quad \text{[Temperature in degrees Kelvin]}$$

Equation 8.

The minimum mean square error algorithm can calculate the constants $a_{r,l}$ assuming that the detector's signal has been acquired for different view and optics temperatures. The number of linear equations that have to be simultaneously solved is $(L+1)(R+1)$. Although Opgal uses a 32-bit floating point arithmetic unit, the accuracy is not adequate for such a task. Therefore we separate the view temperature from the optics influence. Instead of having one single F function, there are several functions $F_{To}(Sig)$ that cover the optics ambient temperature range in small steps of 5 degrees.

$$F_{To}(Sig) = \sum_{l=0}^{L} a_{To,l} \cdot Sig^{l}$$

Equation 9

The optics change in temperature is relatively slow. Consequently, the additional work performed by the digital signal processor (DSP) in order to calculate, by linear interpolation, the required $a_{To,l}$ constants for the new optics temperature is negligible.

3.5 In order to build a real radiometer, additional variables have to be taken into account, such as the target emissivity and ambient temperature influence. However, we would like to mention the influence of the system modulation transfer function (MTF) on temperature measurement accuracy. A given object, at a constant temperature,

will show different temperatures at different distances from the camera. The MTF influence can be compensated, at least for some limited spatial frequency range.

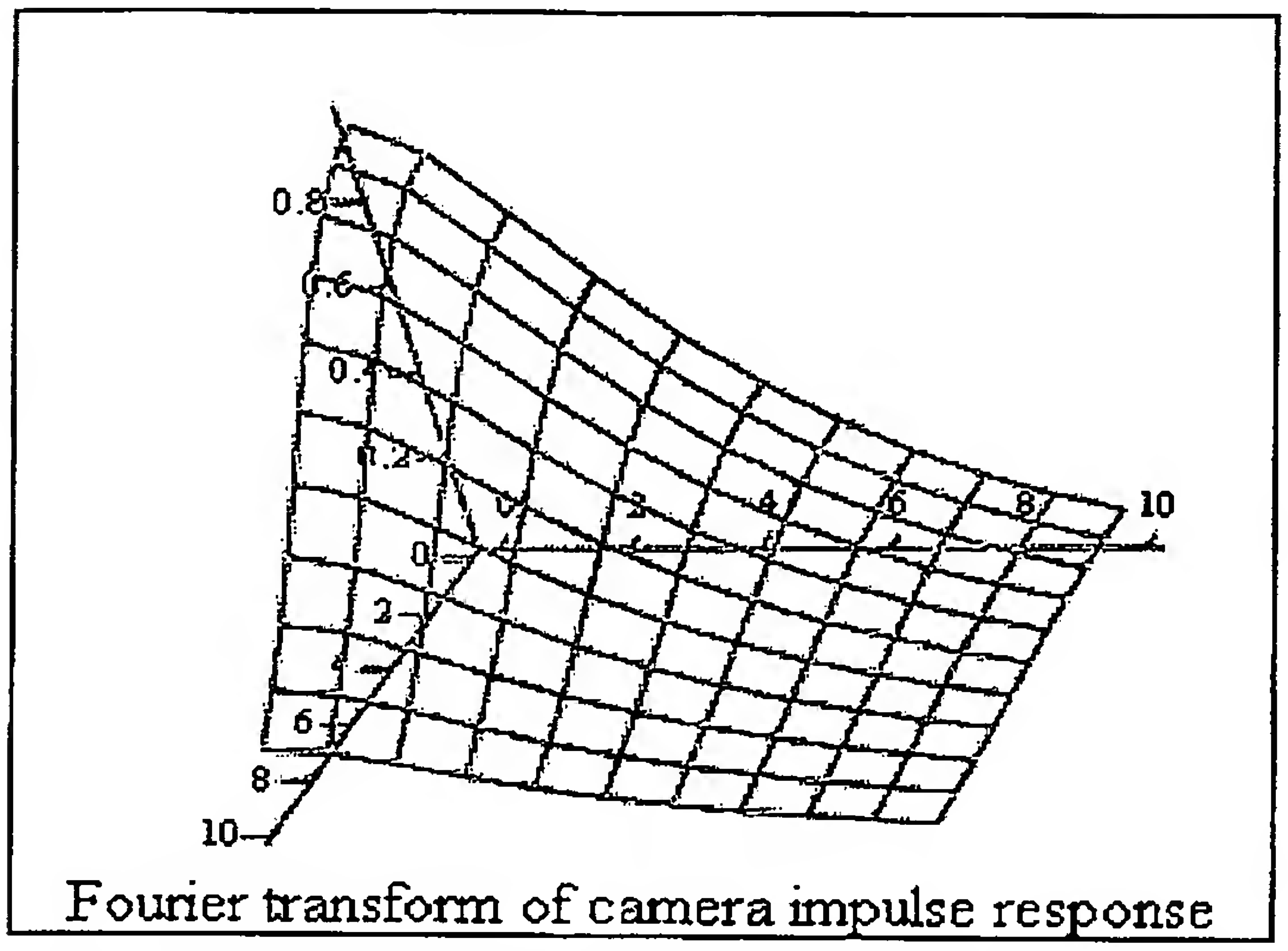

Figure 11. Fourier transform of camera impulse response in cycles per mm, including optics detector and electronics.

Figure 11 describes a typical two-dimensional Fourier transform of an uncooled microbolometer camera. In order to compensate the MTF degradation versus spatial frequency, an inverse filter to the MTF response was designed and software implemented. Figure 12 represents the high pass frequency response of the filter designed in order to compensate the MTF degradation.

3.6 The ideas described in this paper have been implemented on an instrument design to detect human beings suffering from fever. The instrument is monitoring the face temperature and the areas in the image above some given temperature threshold are flickering. The instrument covers a relatively very small range in temperatures between 30 to 42 degrees Celsius within an accuracy of ±0.25 degrees Celsius.

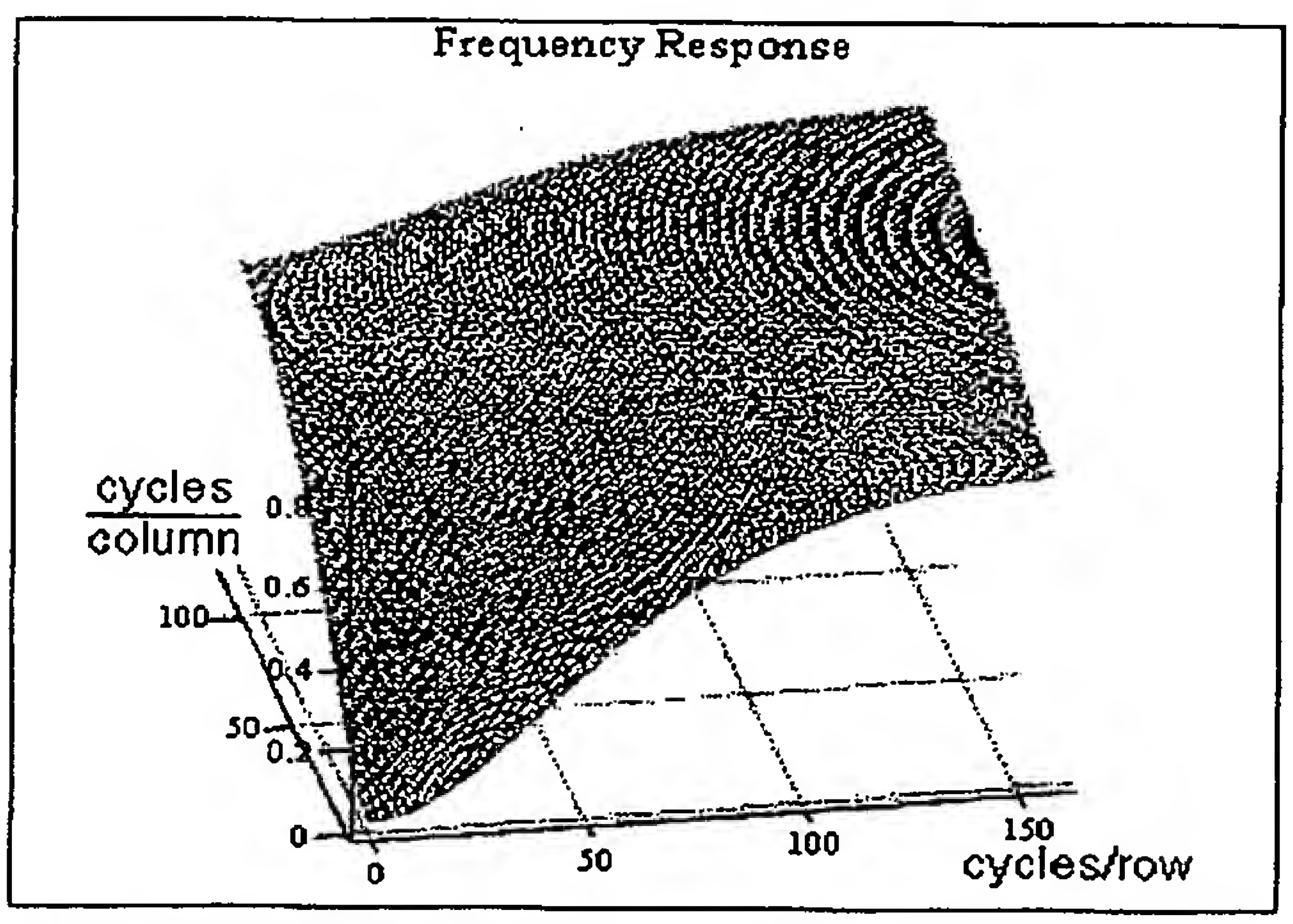

High Pass Filter Frequency Response. This filter is the MTF inverse approximation for a detector that contains 320 by 240 elements.

Figure 12. MTF inverse filter.

4 Conclusions

The basic concept of temperature measurement using a regular uncooled microbolometer detector was described in this paper. The additional hardware required for the temperature measurement capability is really limited and inexpensive. Opgal expects that the capability to measure the temperature will expand the applications span of the regular uncooled microbolometer FLIR cameras.

References:

1. 320x240 microbolometer uncooled IRFPA development by J.L. Tissot, SPIE Vol 4130
2. Meteorological influence on aerosol extinction in the 0.2-40 -μm wavelength range, by Bertil Nilsson, APPLIED OPTICS / Vol. 18, No 20/ 15 October 1979
3. Monolithic silicon microbolometer arrays by R.A. Wood, Chapter 3 of Uncooled Infrared Imaging Arrays and Systems, Semiconductors and Semmietals 47, P. W. Kruse and D. D. Skatrud, Academic Press, San Diego 1997
4. Advances in microbolometer focal plane array technology at Boeing, by P. E. Howard et al. Proc.SPIE Vol. 3379 Infrared Detectors and Focal Plane Arrays 1998.
5. 320X240 microbolometer uncooled IRFPA by E. Mottin et al., Proc. SPIE Vol. 4028, Infrared Detectors and Focal Plane Arrays VI 2000.
6. Uncooled amorphous silicon technology : high performance achievement and future trends by E. Mottin, A. Bain, J.L. Martin, J.L. Ouvrier-Buffet, J.J Yon, J.P. Chatard, J.L. Tissot SPIE Vol 4721
7. Camera for landing applications, by Grimberg Ernest, Proceedings SPIE, Volume 4363, April 2001
8. Optics and dewar head temperature influence on FLIR performances, by Ernest Grimberg SPIE volume 4820 Infrared Technology and Applications XXVIII
9. Digital Filters and their Applications, by V. Cappellini, A. G. Constantinides and P. Emiliani, ACADEMIC PRESS ,1978

10. *Author- Ernest Grimberg phone 972-4-9953981, fax 972-4-9953983, res. phone 972-4-8720694, email address grimberg@opgal.com , P. O. Box 462, Industrial Area, Karmiel 20101, ISRAEL.

 Exhibit B

Geoff Melnick

From: G. E. Ehrlich (1995) Ltd. [patents@ipatent.co.il]

Sent: יום חמישי 07 אוגוסט 2003 17:14

To: Geoff Melnick

Subject: Fw: OPG 1

fyi (nicole)

Tania Hellman de Picciotto
Office Manager and Chief Paralegal
EHRLICH & PARTNERS
G. E. Ehrlich (1995) Ltd.
Ayalon Tower, 15th Floor,
11 Menachem Begin Street, 52 521 Ramat Gan, Israel
Tel.: 03-6127676 Fax.: 03-6127575
My address: tania@ipatent.co.il
Our Website: www.ipatent.co.il

Alliance: Granot, Strauss, Adar & Co. - Website: www.granot-law.co.il

----- Original Message -----
From: Jonathan Zohn [ELOP]
To: 'jeoff@ipatent.co.il'
Sent: 07 August, 2003 03:11 PM
Subject: OPG 1

Attached is a marked version for filing. Please include the changes.

I did not erase the changes in the claims but I think that they narrow the scope and not needed at this time, although they are correct for the final application

Pls comment <<UN OPG 1 draft for filing_corrected_version.doc>>

Jonathan Zohn
Corporate I P Manager
Elbit Systems group

Geoff Melnick

From: Jonathan Zohn [ELOP] [el14012@elop.co.il]
Sent: יום חמישי 07 אוגוסט 2003 19:33
To: 'Geoff Melnick'
Subject: RE: OPG 1

I really had something like that in mind.
claim 3: a flag will be better than the flag

O K TO FILE IN THE IPO

in the name of OPGAL Ltd.

Jonathan Zohn

I P Manager

-----Original Message-----
From: Geoff Melnick [mailto:geoff@ipatent.co.il]
Sent: Thursday, August 07, 2003 7:23 PM
To: Jonathan Zohn [ELOP]
Subject: RE: OPG 1

Hi Jonathan,

Attached please find my revisions to the claims.

What I have done is removed the additions from claim 1 and written them out as separate dependent claims. That way you get the best of both worlds. It is clearly written out but doesn't limit.

Geoffrey. L. Melnick
Patent Attorney
EHRLICH & PARTNERS
G. E. Ehrlich (1995) Ltd.
Ayalon Tower, 15th Floor,
11 Menachem Begin Street, 52 521 Ramat Gan, Israel
Tel.: 03-6127676 Fax.: 03-6127575 Mobile 054 962625 Home 08 936 2304
My address: geoff@ipatent.co.il
Our Website: www.ipatent.co.il

Alliance: Granot, Strauss, Adar & Co. - Website: www.granot-law.co.il